Regulation of Microbe-Associated Molecular Pattern-Induced Hypersensitive Cell Death, Phytoalexin Production, and Defense Gene Expression by Calcineurin B-Like Protein-Interacting Protein Kinases, OsCIPK14/15, in Rice Cultured Cells[1][W][OA]

Takamitsu Kurusu[2], Jumpei Hamada[2], Hiroshi Nokajima, Youichiro Kitagawa, Masahiro Kiyoduka, Akira Takahashi, Shigeru Hanamata, Ryoko Ohno, Teruyuki Hayashi, Kazunori Okada, Jinichiro Koga, Hirohiko Hirochika, Hisakazu Yamane, and Kazuyuki Kuchitsu*

Department of Applied Biological Science, Tokyo University of Science, Noda, Chiba 278–8510, Japan (T.K., J.H., H.N., Y.K., M.K., S.H., R.O., T.H., K.K.); Plant Disease Resistance Research Unit (A.T.) and Division of Genome and Biodiversity Research (H.H.), National Institute of Agrobiological Sciences, Ibaraki 305–8602, Japan; Laboratory of Environmental Biochemistry, Biotechnology Research Center, University of Tokyo, Tokyo 113–8657, Japan (K.O., H.Y.); and Food and Health Research and Development Laboratories, Meiji Seika Kaisha, Ltd., Sakado, Saitama 350–0289, Japan (J.K.)

Although cytosolic free Ca^{2+} mobilization induced by microbe/pathogen-associated molecular patterns is postulated to play a pivotal role in innate immunity in plants, the molecular links between Ca^{2+} and downstream defense responses still remain largely unknown. Calcineurin B-like proteins (CBLs) act as Ca^{2+} sensors to activate specific protein kinases, CBL-interacting protein kinases (CIPKs). We here identified two *CIPK*s, *OsCIPK14* and *OsCIPK15*, rapidly induced by microbe-associated molecular patterns, including chitooligosaccharides and xylanase (*Trichoderma viride*/ethylene-inducing xylanase [TvX/EIX]), in rice (*Oryza sativa*). Although they are located on different chromosomes, they have over 95% nucleotide sequence identity, including the surrounding genomic region, suggesting that they are duplicated genes. OsCIPK14/15 interacted with several OsCBLs through the FISL/NAF motif in yeast cells and showed the strongest interaction with OsCBL4. The recombinant OsCIPK14/15 proteins showed Mn^{2+}-dependent protein kinase activity, which was enhanced both by deletion of their FISL/NAF motifs and by combination with OsCBL4. *OsCIPK14/15-RNAi* transgenic cell lines showed reduced sensitivity to TvX/EIX for the induction of a wide range of defense responses, including hypersensitive cell death, mitochondrial dysfunction, phytoalexin biosynthesis, and pathogenesis-related gene expression. On the other hand, TvX/EIX-induced cell death was enhanced in *OsCIPK15*-overexpressing lines. Our results suggest that OsCIPK14/15 play a crucial role in the microbe-associated molecular pattern-induced defense signaling pathway in rice cultured cells.

Calcium ions regulate diverse cellular processes in plants as a ubiquitous internal second messenger, conveying signals received at the cell surface to the inside of the cell through spatial and temporal concentration changes that are decoded by an array of Ca^{2+} sensors (Reddy, 2001; Sanders et al., 2002; Yang and Poovaiah, 2003). Several families of Ca^{2+} sensors have been identified in higher plants. The best known are calmodulins (CaMs) and CaM-related proteins, which typically contain four EF-hand domains for Ca^{2+} binding (Zielinski, 1998). Unlike mammals, which possess single molecular species of CaM, plants have at least three distinct molecular species of CaM playing diverse physiological functions and whose expression is differently regulated (Yamakawa et al., 2001; Luan et al., 2002; Karita et al., 2004; Takabatake et al., 2007). The second major class is exemplified by the Ca^{2+}-dependent protein kinases, which contain CaM-like Ca^{2+}-binding domains and a kinase domain in a single protein (Harmon et al., 2000). In addition, a new family of Ca^{2+} sensors was identified as calcineurin B-like (CBL) proteins, which consists of proteins similar to

[1] This work was supported by the Ministry of Education, Science, Culture, Sports and Technology of Japan (Grant-in-Aid for Scientific Research on Innovative Areas no. 21200067 to T.K., Grant-in-Aid for Exploratory Research no. 21658118 to K.K., Grant-in-Aid for Young Scientists [B] no. 21780041 to T.K.), and by the Ministry of Agriculture, Forestry and Fisheries of Japan (Integrated Research Project for Plants, Insects, and Animals Using Genome Technology grant no. MP–2134 to K.K.).

[2] These authors contributed equally to the article.

* Corresponding author; e-mail kuchitsu@rs.noda.tus.ac.jp.

The author responsible for distribution of materials integral to the findings presented in this article in accordance with the policy described in the Instructions for Authors (www.plantphysiol.org) is: Kazuyuki Kuchitsu (kuchitsu@rs.noda.tus.ac.jp).

[W] The online version of this article contains Web-only data.

[OA] Open Access articles can be viewed online without a subscription.

www.plantphysiol.org/cgi/doi/10.1104/pp.109.151852

both the regulatory β-subunit of calcineurin and the neuronal Ca^{2+} sensor in animals (Liu and Zhu, 1998; Kudla et al., 1999).

Unlike CaMs, which interact with a large variety of target proteins, CBLs specifically target a family of protein kinases referred to as CBL-interacting protein kinases (CIPKs) or SnRK3s (for sucrose nonfermenting 1-related protein kinases type 3), which are most similar to the SNF family protein kinases in yeast (Luan et al., 2002). A database search of the Arabidopsis (*Arabidopsis thaliana*) genome sequence revealed 10 *CBL* and 25 *CIPK* homologues (Luan et al., 2002). Expression patterns of these Ca^{2+} sensors and protein kinases suggest their diverse functions in different signaling processes, including light, hormone, sugar, and stress responses (Batistic and Kudla, 2004). AtCBL4/Salt Overly Sensitive3 (SOS3) and AtCIPK24/SOS2 have been shown to play a key role in Ca^{2+}-mediated salt stress adaptation (Zhu, 2002). The CBL-CIPK system has been shown to be involved in signaling pathways of abscisic acid (Kim et al., 2003a), sugar (Gong et al., 2002a), gibberellins (Hwang et al., 2005), salicylic acid (Mahajan et al., 2006), and K^+ channel regulation (Li et al., 2006; Lee et al., 2007; for review, see Luan, 2009; Batistic and Kudla, 2009). However, physiological functions of most of the family members still remain largely unknown.

Plants respond to pathogen attack by activating a variety of defense responses, including the generation of reactive oxygen species (ROS), synthesis of phytoalexins, expression of pathogenesis-related (PR) genes, cell cycle arrest, and mitochondrial dysfunction followed by a form of hypersensitive cell death known as the hypersensitive response (Nürnberger and Scheel, 2001; Greenberg and Yao, 2004; Kadota et al., 2004b). Transient membrane potential changes and Ca^{2+} influx are involved at the initial stage of defense responses (Kuchitsu et al., 1993; Pugin et al., 1997; Blume et al., 2000; Kadota et al., 2004a). Many kinds of defense responses are prevented when Ca^{2+} influx is compromised by Ca^{2+} chelators (Nürnberger and Scheel, 2001; Lecourieux et al., 2002). Since complex spatiotemporal patterns of cytosolic free Ca^{2+} concentration have been suggested to play pivotal roles in defense signaling (Nürnberger and Scheel, 2001; Sanders et al., 2002), multiple Ca^{2+} sensor proteins and their effectors should function in the defense signaling pathways. Although possible involvement of some CaM isoforms (Heo et al., 1999; Yamakawa et al., 2001), Ca^{2+}-dependent protein kinases (Romeis et al., 2000, 2001; Ludwig et al., 2005; Kobayashi et al., 2007; Yoshioka et al., 2009), as well as Ca^{2+} regulation of EF-hand-containing enzymes such as ROS-generating NADPH oxidase (Ogasawara et al., 2008) have been suggested, other Ca^{2+}-regulated signaling components still remain to be identified. No CBLs or CIPKs have so far been implicated as signaling components in defense signaling.

N-Acetylchitooligosaccharides, chitin fragments, are microbe-associated molecular patterns (MAMPs) that are recognized by plasma membrane receptors (Kaku et al., 2006; Miya et al., 2007) and induce a variety of defense responses, such as membrane depolarization (Kuchitsu et al., 1993; Kikuyama et al., 1997), ion fluxes (Kuchitsu et al., 1997), ROS production (Kuchitsu et al., 1995), phytoalexin biosynthesis (Yamada et al., 1993), and induction of PR genes (Nishizawa et al., 1999), without hypersensitive cell death in rice (*Oryza sativa*) cells. In contrast, a fungal proteinaceous elicitor, xylanase from *Trichoderma viride* (TvX)/ethylene-inducing xylanase (EIX), which is recognized by two putative plasma membrane receptors, LeEix1 and LeEix2 (Ron and Avni, 2004), triggers hypersensitive cell death along with different kinetics of ROS production and activation of a mitogen-activated protein kinase, OsMPK6, previously named as OsMPK2 or OsMAPK6, in rice cells (Kurusu et al., 2005). These two fungal MAMPs thus provide excellent model systems to study innate immunity in rice cells.

This study identified two *CIPK*s involved in various MAMP-induced layers of defense responses, including PR gene expression, phytoalexin biosynthesis, mitochondrial dysfunction, and cell death, in rice. Molecular characterization of these CIPKs, including interaction with the putative Ca^{2+} sensors as well as their physiological functions, is discussed.

RESULTS

Identification of *CIPK*s Induced by MAMPs

A database search of the rice genome sequence revealed 30 *CIPK* homologues (Kolukisaoglu et al., 2004). As a first step toward elucidating the molecular mechanisms of CBL-CIPKs in defense signaling, the expression patterns of several *CIPK* genes were surveyed in suspension-cultured rice cells in response to several MAMPs by semiquantitative reverse transcription (RT)-PCR analyses. The expression levels of two CIPK family members, *OsCIPK14* and *OsCIPK15*, were greatly enhanced by *N*-acetylchitoheptaose and TvX/EIX, while those of other *CIPK*s, such as *OsCIPK2*, *OsCIPK10*, *OsCIPK11*, *OsCIPK12*, and *OsCIPK19* (accession nos. AK072868, AK066541, AK103032, AK101442, and AK069486, respectively), did not show significant changes (Supplemental Fig. S1).

The full-length cDNAs of *OsCIPK14* (GenBank accession no. AB264036) and *OsCIPK15* (accession no. AB264037), which encoded polypeptides of 439 and 434 amino acids, respectively, were obtained using RACE-PCR (Supplemental Fig. S2). *OsCIPK14* and *OsCIPK15* did not have introns and were located on different chromosomes (*OsCIPK14* on chromosome 12 and *OsCIPK15* on chromosome 11). They had over 95% nucleotide sequence identity even in the surrounding noncoding regions of the genome. The predicted amino acid sequences of OsCIPK14 and OsCIPK15 were almost identical and differed in only a single amino acid substitution except for the five additional amino acids (Supplemental Fig. S2). These results

suggest that *OsCIPK14* and *OsCIPK15* are duplicated genes.

OsCIPK14/15 showed 44% homology with AtCIPK24/SOS2 at the amino acid level (Liu et al., 2000). Amino acid sequences of the N terminus of the kinase domain and the FISL/NAF motif (Albrecht et al., 2001) were especially well conserved (Supplemental Fig. S2).

Spatiotemporal Expression Patterns of *OsCIPK14/15*

MAMP-induced accumulation of *OsCIPK14* and *OsCIPK15* mRNAs was analyzed by real-time RT-PCR analyses. Because OsCIPK14 and OsCIPK15 are so similar, their expression pattern could not be discriminated by RT-PCR analyses. The expression of *OsCIPK14/15* was up-regulated at 2 h by both TvX/EIX and *N*-acetylchitoheptaose (Fig. 1A). The time course of induction of *OsCIPK14/15* was more rapid and transient than that of a PR gene, *Probenazole-Inducible Gene1* (*PBZ1*)/*PR10a* (accession no. D38170; Midoh and Iwata, 1996; Fig. 1B). These results were confirmed by northern-blot analyses (Supplemental Fig. S3A).

Tissue-specific expression of *OsCIPK14/15* genes in shoots and roots of 7-d-old seedlings, mature leaves, and cultured cells was analyzed by northern hybridization. The *OsCIPK14/15* mRNAs were expressed throughout the plants in seedlings as well as in cultured cells and were most abundant in aerial parts of seedlings (Supplemental Fig. S3B).

Interaction of OsCIPK14/15 with OsCBLs

A database search of the rice genome sequence revealed 10 *CBL* homologues, which are categorized as several subgroups by phylogenic analyses (Kolukisaoglu et al., 2004). We picked up six OsCBLs from several subgroups (*OsCBL2*, accession no. J033068L17; *OsCBL3*, J033133I20; *OsCBL4*, J033035L13; *OsCBL5*, J013071C24; *OsCBL6*, J013001C11; *OsCBL9*, J023045O14) and tested possible interaction with OsCIPK14/15 by the yeast two-hybrid method. The *OsCIPK14* and *OsCIPK15* genes were fused to the *GAL4*-binding domain, and six OsCBLs were fused to the *GAL4* activation domain. Figure 2, A and C, shows the growth of yeast cells on the selection medium and the corresponding β-galactosidase assay when OsCIPK14/15 and OsCBLs were used as bait and prey, respectively. OsCIPK14 and OsCIPK15 interacted with several OsCBLs (OsCBL2, OsCBL3, OsCBL4, OsCBL5, and OsCBL6) but not with OsCBL9 and showed the strongest interaction with OsCBL4 (Fig. 2, A, C, and D). Interestingly, the expression of the *OsCBL4* gene was also induced upon elicitation, while *OsCBL9* was not (Supplemental Fig. S5).

The FISL/NAF motif is highly conserved in both OsCIPK14 and OsCIPK15 proteins (Supplemental Fig. S2). This domain of the CIPK family has been shown to interact with CBLs (Albrecht et al., 2001) and to possess autoinhibitory function (Guo et al., 2001; Gong et al., 2002a). Mutant proteins (OsCIPK14/15DF) deficient in the FISL/NAF motif were generated (Supplemental Fig. S6). OsCIPK14DF and OsCIPK15DF failed to interact with OsCBLs in yeast (Figure 2, B–D), suggesting that the FISL/NAF motif in OsCIPK14/15 is crucial for interaction with OsCBLs, and this interaction mechanism between CIPKs and CBLs is highly conserved among plant species.

The presence of conserved EF-hand motifs in OsCBLs suggests that they may bind Ca^{2+}. To test the Ca^{2+}-binding activity of OsCBLs, Ca^{2+}-induced electrophoretic mobility shift analyses were carried out.

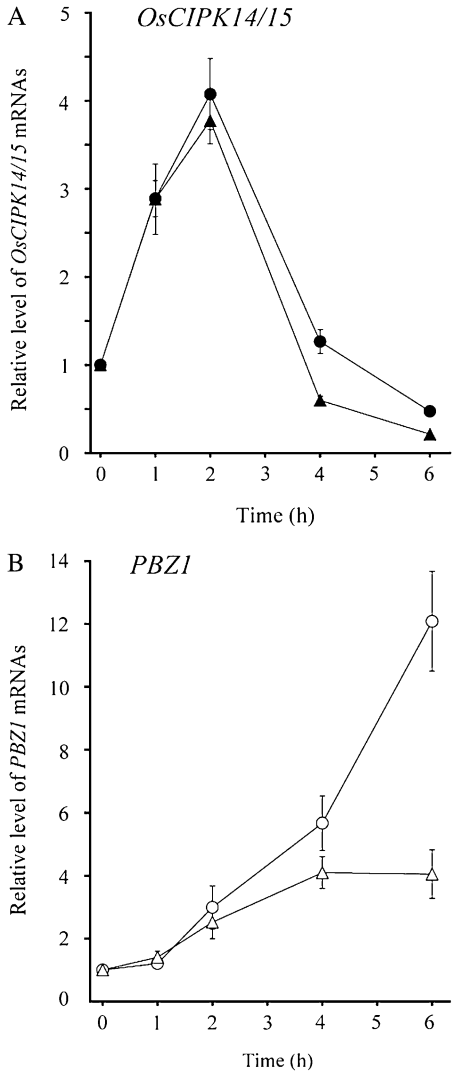

Figure 1. Induction of *OsCIPK14/15* genes in response to MAMPs. mRNA accumulations of *OsCIPK14/15* (A) and *PBZ1* (B) in TvX/EIX-treated (circles) or *N*-acetylchitoheptaose-treated (triangles) cells. Total RNA was isolated from rice cells harvested at the indicated time points of TvX/EIX (60 μg mL^{-1}) or *N*-acetylchitoheptaose (1 μM) treatment. The amount of each mRNA was calculated from the threshold point located in the log-linear range of RT-PCR. The relative level of each gene in the control cells at time 0 was standardized as 1. The error bars indicate SD of four experiments.

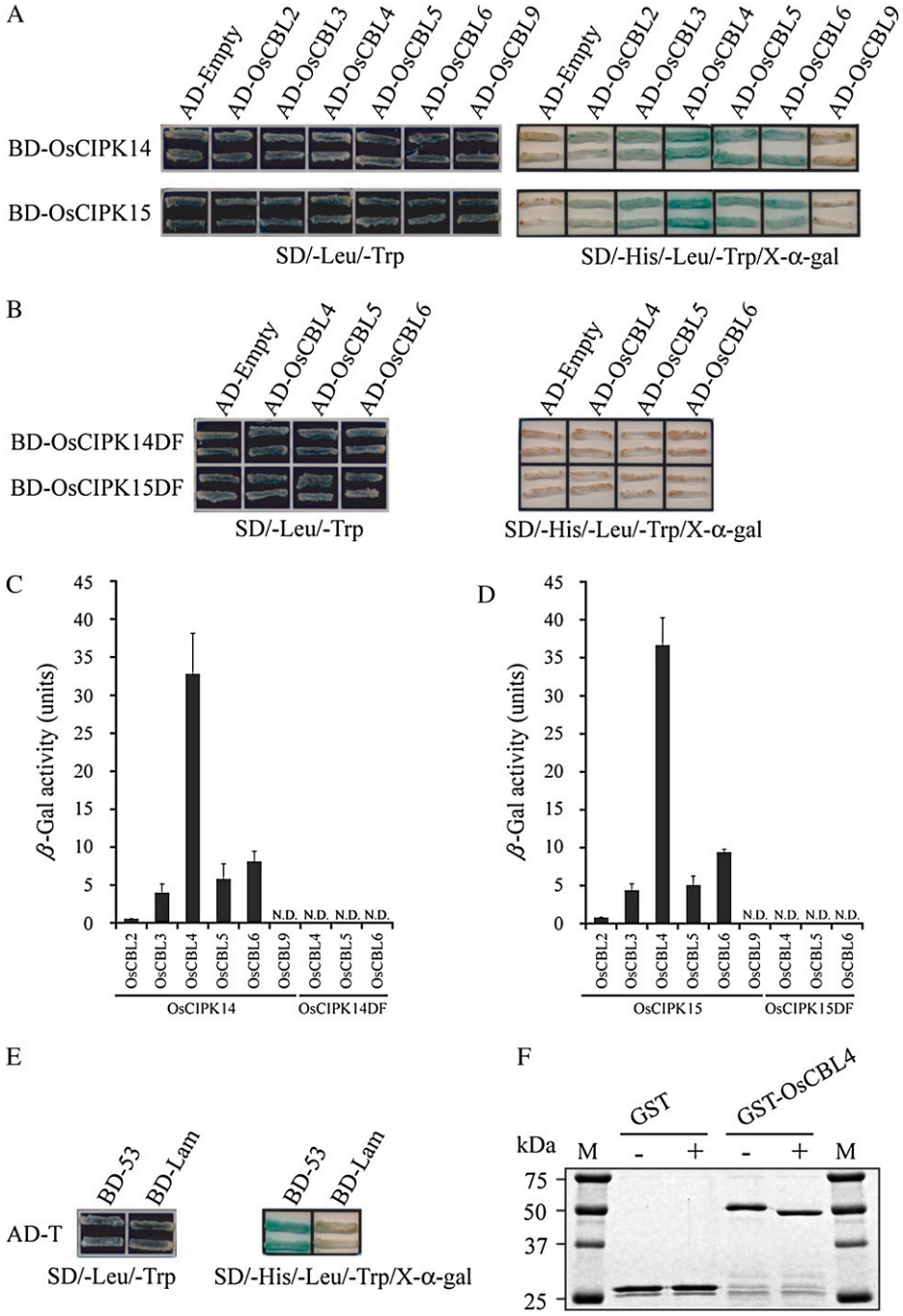

Figure 2. OsCIPK14 and OsCIPK15 interact with OsCBLs in a yeast two-hybrid system. A and B, OsCIPK14/15 (A) or OsCIPK14/15DF (B) was fused to the GAL4 DNA-binding domain (BD) and OsCBLs were fused to the GAL4 activation domain (AD). Nutritional reporter systems minus Leu and Trp (SD/−Leu/−Trp) and minus Leu, Trp, and His plus X-α-Gal (SD/−His/−Leu/−Trp/X-α-gal) were employed to examine the interaction between OsCIPK14/15 and OsCBLs (A) or OsCIPK14/15DF and OsCBLs (B). C and D, Quantitative β-galactosidase activity of combinations between OsCIPK14/14DF and OsCBLs (C) or OsCIPK15/15DF and OsCBLs (D). N. D., Not detected. Average values and SE of three independent experiments are shown. E, A positive or negative control showing the interaction between SV40 large T-antigen (T) and murine p53 (53) or SV40 large T-antigen and human lamin C (Lam), respectively. F, Ca^{2+}-induced electrophoretic mobility shift analysis of GST-OsCBL4 fusion protein. A total of 2.7 μg of protein (GST or GST-OsCBL4) was incubated with 2 mM EDTA (−) or $CaCl_2$ (+), subjected to 12.5% SDS-PAGE, and stained with Coomassie Brilliant Blue. The molecular masses of standard makers are indicated in kD in the M lane.

Ca^{2+}-binding proteins such as CaM bind Ca^{2+} in the presence of SDS and show higher electrophoretic mobility than in the absence of free Ca^{2+} (Zielinski, 2002). Recombinant glutathione *S*-transferase (GST)-OsCBL4 fusion proteins, which showed the strongest interaction with OsCIPK14/15, were expressed in *Escherichia coli* and partially purified using glutathione-Sepharose columns. OsCBL4 displayed a characteristic electrophoretic mobility shift when incubated with 2 mM $CaCl_2$ prior to electrophoresis, while the mobility shift was not observed for GST protein as a control (Fig. 2F). These results suggest that OsCBL4 binds Ca^{2+} to function as a putative Ca^{2+} sensor.

Regulation of the Protein Kinase Activity of OsCIPK14 and OsCIPK15

To characterize the biochemical properties of OsCIPK14 and OsCIPK15, recombinant GST-OsCIPK14 and GST-OsCIPK15 fusion proteins were expressed in *E. coli* and partially purified using glutathione-Sepharose columns. Proteins of the expected size (78 kD for

GST-OsCIPK14 and 77.4 kD for GST-OsCIPK15) were detected by SDS-PAGE (top bands in Fig. 3A), both of which showed autophosphorylation activity in the presence of Mn^{2+} but not of other divalent cations such as Mg^{2+} or Ca^{2+} (Fig. 3A), suggesting that Mn^{2+} functions as a cofactor for OsCIPK14/15. These biochemical properties of the recombinant OsCIPK14/15 are similar to those of other CIPKs in other plant species (Shi et al., 1999; Gong et al., 2002b; Kim et al., 2003b). The bottom bands shown in Figure 3A seemed to correspond to the degraded forms of GST-OsCIPK14/15 proteins.

In Arabidopsis, the FISL/NAF motif of CIPKs possess autoinhibitory function and CIPKs are activated by binding of CBLs via the FISL/NAF motif in a Ca^{2+}-dependent manner (Halfter et al., 2000; Guo et al., 2001; Gong et al., 2002a). To investigate whether the kinase activity of OsCIPK14/15 was modulated by interaction with OsCBLs, the autophosphorylation activity in the presence or absence of OsCBLs was

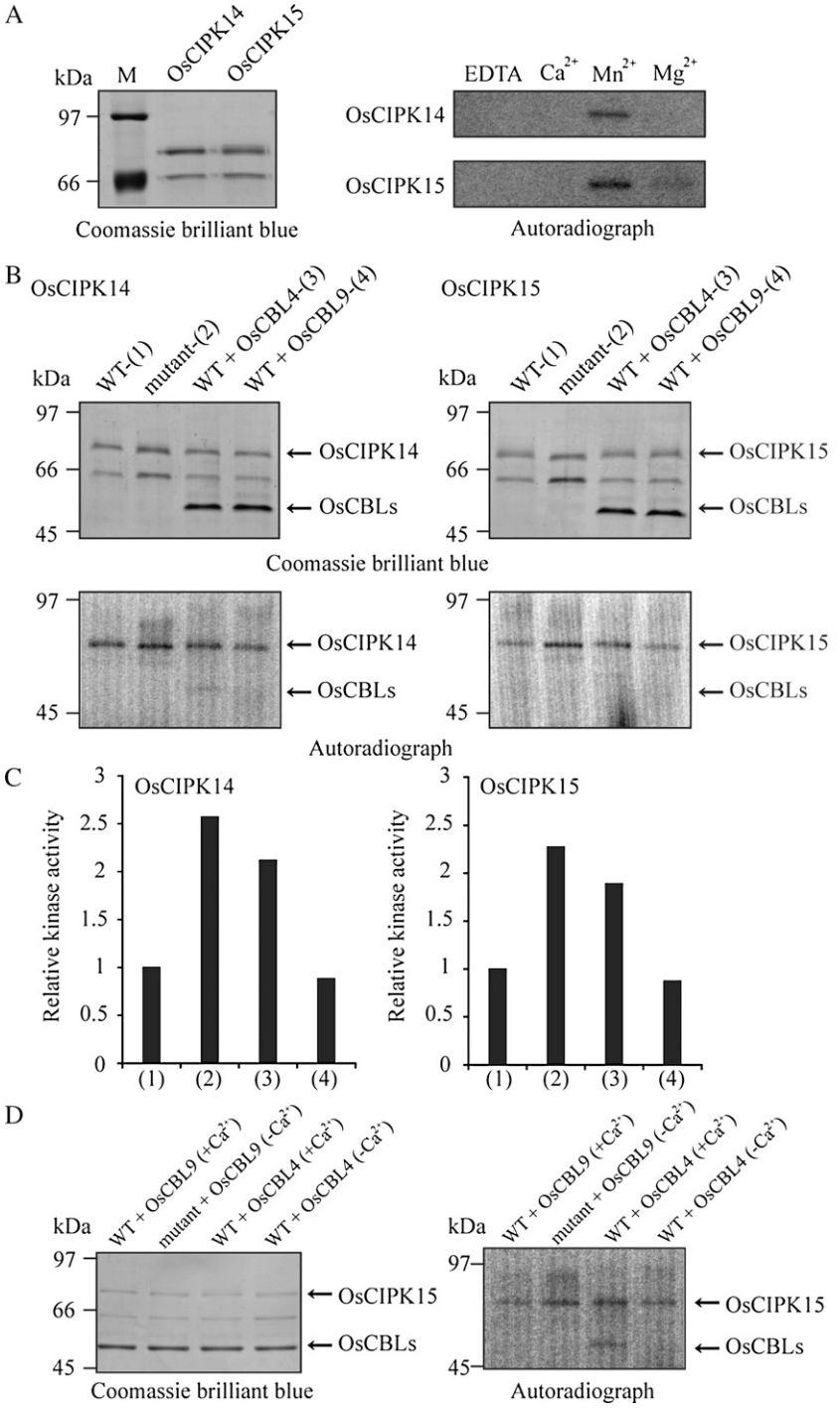

Figure 3. Purification of OsCIPK14/15 and OsCBL proteins and their activation mechanism. A, Purification of recombinant (GST-OsCIPK14 and GST-OsCIPK15) proteins visualized by Coomassie Brilliant Blue staining. The molecular masses of standard markers are indicated in kD in the M lane. Autophosphorylation activity and cofactor dependence of GST-OsCIPK14 and GST-OsCIPK15 are shown. Aliquots of the fusion proteins (100 ng) were incubated with [γ-^{32}P]ATP in the presence of EDTA, $CaCl_2$, $MnCl_2$, or $MgCl_2$ at a concentration of 5 mM. B, Purification of GST-OsCIPK14/15, GST-OsCIPK14/15DF mutants, GST-OsCBL4, and GST-OsCBL9 visualized by Coomassie Brilliant Blue staining. For autophosphorylation activity of OsCIPK14/15 in the presence of OsCBLs, aliquots of GST-OsCIPK14/15 or GST-OsCIPK14DF/15DF fusion proteins (100 ng) in the presence or absence of GST-OsCBL4 and GST-OsCBL9 fusion proteins (200 ng) were incubated in the kinase assay buffer ([γ-^{32}P]ATP, 20 mM Tris-HCl, pH 8.0, 1 mM DTT, 5 mM $MnCl_2$, and 1 mM $CaCl_2$). C, The activation levels of OsCIPK14/15 and OsCIPK14DF/15DF mutants. The relative activation levels of OsCIPK14 and OsCIPK15 were standardized as 1. Column 1, Wild-type (WT) CIPK; column 2, mutant CIPK; column 3, wild-type CIPK + OsCBL4; column 4, wild-type CIPK + OsCBL9. D, Calcium-dependent autophosphorylation activity of OsCIPK15 by OsCBL4. Aliquots of GST-OsCIPK15 or GST-OsCIPK15DF fusion proteins (100 ng) in the presence of GST-OsCBL4 and GST-OsCBL9 fusion proteins (600 ng) were incubated in the kinase assay buffer ([γ-^{32}P]ATP, 20 mM Tris-HCl, pH 8.0, 1 mM DTT, and 5 mM $MnCl_2$, with or without 1 mM $CaCl_2$).

analyzed using an in vitro kinase assay. The autophosphorylation activity of OsCIPK14/15 was enhanced by GST-OsCBL4 in the presence of Mn^{2+} and Ca^{2+} (Fig. 3, B and C) but not in the absence of Ca^{2+} in the reaction buffer (Fig. 3, B–D). The autophosphorylation activity of OsCIPK14/15 was not affected by OsCBL9 (Fig. 3, B and C), which did not show an interaction with OsCIPK14/15 (Fig. 2, A and C).

A CBL from pea (*Pisum sativum*) has been reported to be phosphorylated by PsCIPK (Mahajan et al., 2006). Phosphorylation of OsCBL4 by OsCIPK14/15 was also detected in the presence of Mn^{2+}, Ca^{2+}, and a substantial amount of OsCBL4 protein (Fig. 3D).

To assess the roles of the FISL motif of OsCIPK14/15, a recombinant mutant protein of OsCIPK14/15 defective in the FISL/NAF motif, GST-OsCIPK14/15DF (Supplemental Fig. S6), was expressed in *E. coli* and partially purified (Fig. 3B). The mutant protein showed higher autophosphorylation activity than the wild-type protein (Fig. 3, B and C). Exogenous Ca^{2+} showed no effect on the autophosphorylation activity of either GST-OsCIPK14/15 (Fig. 3A) or GST-OsCIPK15DF (Fig. 3D). These results indicate that the protein kinase activity of OsCIPK14/15 is negatively regulated by its FISL/NAF motif. The autoinhibitory function of OsCIPK14/15 may be canceled by Ca^{2+}-dependent binding of OsCBL4 via the FISL/NAF motif.

Suppression of MAMP-Induced Mitochondrial Dysfunction and Hypersensitive Cell Death in the *OsCIPK14/15-RNAi* Lines

Since *OsCIPK14* and *OsCIPK15* are duplicated genes, their translated products may be functionally redundant. To reveal the physiological roles of OsCIPK14 and OsCIPK15, transgenic cell lines were generated in which the expression of both *OsCIPK14* and *OsCIPK15* was suppressed by RNA interference (RNAi) using gene-specific sequences (340 bp of the 3′ untranslated region of *OsCIPK14*). Five independent transgenic cell lines were generated by means of *Agrobacterium tumefaciens*-mediated transformation. Nontransgenic cells were investigated simultaneously as a control, whose transduced genes were removed by heterozygous segregation. RT-PCR and real-time RT-PCR analyses revealed significant reductions in *OsCIPK14/15* mRNA levels in comparison with the control (Fig. 4, A and B). The expression of the most closely related homolog, *OsCIPK11* (Kolukisaoglu et al., 2004), was not affected (Fig. 4A), indicating that only the transcripts of *OsCIPK14/15* were specifically reduced.

A series of TvX/EIX-induced defense responses were compared between the wild-type and *OsCIPK14/15-RNAi* lines (Fig. 4–7). Evans blue staining was applied to quantify the levels of cell death. Hypersensitive cell

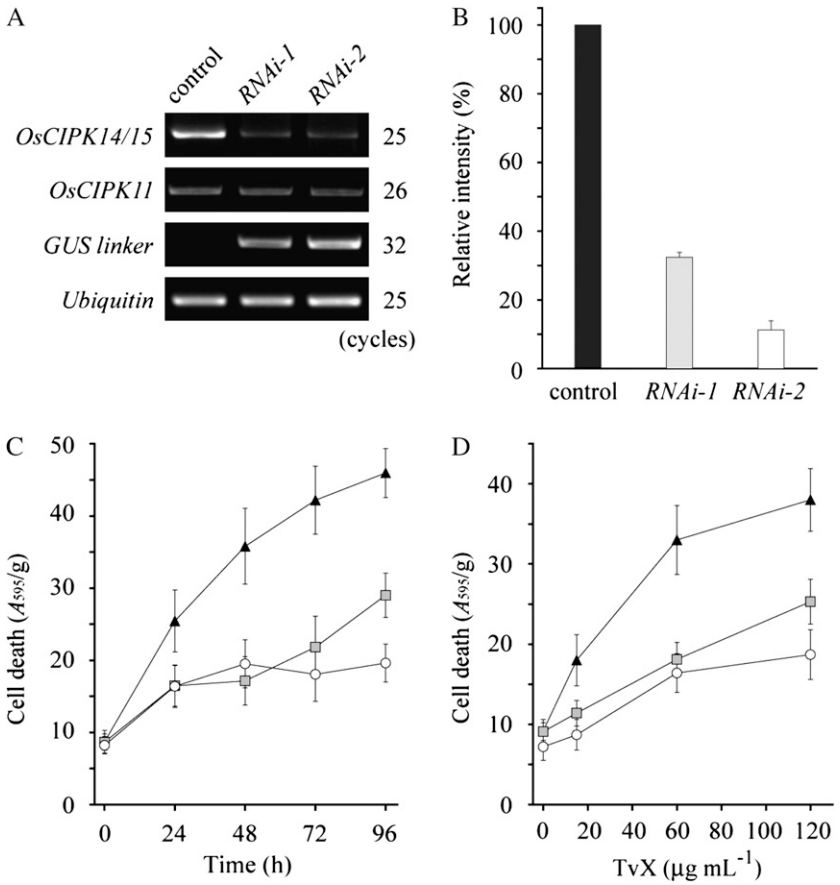

Figure 4. Effects of *OsCIPK14/15* suppression on TvX/EIX elicitor-induced hypersensitive cell death. A, RT-PCR analysis of *OsCIPK14/15* in two independent *RNAi* lines. The expression of *OsCIPK11*, the most closely related gene to *OsCIPK14/15*, was examined as a control experiment. The expression of *GUS* linker indicates RT-PCR products of the *GUS* linker region, indicative of the expression of the trigger double-stranded RNA. *Ubiquitin* cDNA was used as an internal control. PCR products were analyzed by agarose gel electrophoresis. B, Quantitative expression levels of *OsCIPK14/15* mRNAs in the *OsCIPK14/15-RNAi* lines by real-time quantitative PCR. The amounts of *OsCIPK14/15* mRNAs were calculated from the threshold point located in the log-linear range of RT-PCR. The relative level of the *OsCIPK14/15* mRNAs in the control cells was standardized as 100%. The error bars indicate SD of three experiments. C, Time course of cell death after TvX/EIX treatment (120 μg mL^{-1}) of the *OsCIPK14/15-RNAi* lines. D, TvX/EIX-induced dose-dependent cell death in the *OsCIPK14/15-RNAi* lines. Rice cells were tested at 72 h after the addition of the TvX/EIX elicitor at various concentrations. Evans blue staining was applied to quantify the level of the TvX/EIX-induced cell death. Average values and SE of three independent experiments for the control line (black triangles) and two independent *RNAi* lines (light gray squares for *RNAi-1* and white circles for *RNAi-2*) are shown. Three other independent *RNAi* lines showed similar results (data not shown).

death was significantly suppressed in the *OsCIPK14/15-RNAi* lines compared with the control, and the levels of cell death corresponded with the expression levels of *OsCIPK14/15* (Fig. 4, B–D).

Increasing evidence suggests the involvement of mitochondrial dysfunction in the induction of hypersensitive cell death in plants as well as in animals (Lam et al., 2001). Reductase activity of 3-(4,5-dimethyl-2-thiazolyl)-2,5-diphenyl-2H tetrazolium bromide (MTT) was monitored as a marker for mitochondrial function (Ikegawa et al., 1998; Yamamoto et al., 2002). TvX/EIX induced a rapid reduction in MTT reductase activity in rice cells (Fig. 5A). Cyclosporine A (CsA) is a potent inhibitor for mitochondrial permeability transition and mitochondria-mediated apoptosis in animals (Marchetti et al., 1996). CsA also inhibits protoporphyrin IX-induced mitochondrial membrane depolarization and cell death in Arabidopsis (Yao et al., 2004). CsA inhibited TvX/EIX-induced reduction in MTT reductase activity (Fig. 5B) and cell death in rice cells (Fig. 5C), suggesting that mitochondrial dysfunction is involved in TvX/EIX-induced hypersensitive cell death.

In addition to the suppression of TvX/EIX-induced cell death (Fig. 4, C and D), reduction in MTT reductase activity was also significantly suppressed in the *OsCIPK14/15-RNAi* lines compared with the control (Fig. 5A). Taken together, these results suggested that OsCIPK14/15 may be involved in the regulation of the MAMP-induced mitochondria-mediated hypersensitive cell death.

Involvement of OsCIPK14/15 in the Regulation of Phytoalexin Biosynthesis

Pharmacological evidence suggests the importance of Ca^{2+} in MAMP-induced phytoalexin biosynthesis in rice (Umemura et al., 2002). Quantitative HPLC-tandem mass spectrometry analyses (Shimizu et al., 2008) revealed that TvX/EIX induces the accumulation of momilactones and phytocassanes, which are major phytoalexins in rice (Fig. 6, A and B; Koga et al., 1995, 1997). In the *OsCIPK14/15-RNAi* cells, the accumulation of both momilactones and phytocassanes was impaired significantly (Fig. 6, A and B).

In rice, *ent*-copalyl diphosphate synthase 4 (*OsCPS4/OsCyc1*) and *ent*-kaurene synthase-like 4 (*OsKSL4/OsKS4*) are responsible for the biosynthesis of momilactones and *ent*-copalyl diphosphate synthase 2 (*OsCPS2/OsCyc2*) and *ent*-kaurene synthase-like 7 (*OsKSL7/OsDTC1*) are responsible for the biosynthesis of phytocassanes (accession nos. AB066270, AB126934, AB066271, and AB089272, respectively; Cho et al., 2004; Otomo et al., 2004a, 2004b; Shimizu et al., 2008). Slow and prolonged expression of all these cyclase genes was induced by TvX/EIX, which was significantly suppressed in the *OsCIPK14/15-RNAi* lines (Fig. 6C). Taken together, these results suggest the possible involvement of OsCIPK14/15 in the regulation of TvX/EIX-induced phytoalexin biosynthesis.

Involvement of OsCIPK14/15 in TvX/EIX-Induced PR Gene Expression

To test the possible involvement of OsCIPK14/15 in the regulation of expression of PR genes, the expression of five representative PR genes, *PBZ1/PR10a*, *Chitinase1* (*Cht-1*; accession no. D16221), *EL2* (accession no. D64038), *EL3* (accession no. D64039), and Phe ammonia lyase (*PAL*; accession no. X16099), was examined (Midoh and Iwata, 1996; Minami et al., 1996; Nishizawa et al., 1999) by real-time RT-PCR analyses. Among the five PR genes, TvX/EIX-induced expression of *PBZ1* and *Cht-1* showed slow and prolonged kinetics (Fig. 7A). In the *OsCIPK14/15-RNAi* lines, the initial early phase of induction within a few hours was not affected, while the later prolonged accumulation of the transcripts was suppressed significantly (Fig. 7A).

On the contrary, TvX/EIX-induced expression of *EL2* and *EL3* showed very rapid and transient kinetics and peaked around 30 min, which was not affected by the suppression of *OsCIPK14/15* (Fig. 7B). TvX/EIX also triggered rapid and transient induction of *PAL*. Interestingly, in the *OsCIPK14/15-RNAi* cells, the kinetics of the rapid induction phase of *PAL* was not affected, while the decrease in *PAL* mRNA levels occurred earlier than in the control (Fig. 7C). Since the TvX-induced expression pattern of *OsCIPK14/15* was not earlier than that of *EL2* and *EL3* (Figs. 1A and 7B), OsCIPK14/15 may be involved not in the initial early stage but rather mainly in the later stage of the TvX/EIX-induced transcriptional regulation of PR genes.

Elicitor Sensitivity in Transgenic Cultured Cells Overexpressing *OsCIPK15* and *OsCIPK15DF*

Because these results suggested that the FISL/NAF motif in OsCIPK14/15 is an important element to interact with native rice CBLs that have Ca^{2+}-binding activity (Fig. 2, B and F), it was tested whether the FISL/NAF motif in OsCIPK14/15 is involved in elicitor-induced defense signaling. Transgenic cultured cells overexpressing *OsCIPK15* mRNA were treated with the elicitor, and the resulting hypersensitive cell death and phytoalexin accumulation were studied. The elicitor-induced cell death was much more evident in *OsCIPK15*-overexpressing cells than in *GUS*-expressing control cells, and their cell death corresponded to the *OsCIPK15* expression level in the transgenic cells (Fig. 8, A and B). Moreover, in the *OsCIPK15*-overexpressing line, the accumulation of both momilactones and phytocassanes was much more abundant than in the control line at a low concentration of TvX (Fig. 8C). In contrast to the *OsCIPK15* overexpressors, the levels of TvX-induced hypersensitive cell death in the *OsCIPK15DF* overexpressors were comparable to those in the *GUS* control (Fig. 8, A and B). These results indicate that the overexpression of *OsCIPK15* enhanced sensitivity to the TvX elicitor and that the FISL/NAF motif is an essential component in the MAMP-triggered signal transduction pathway.

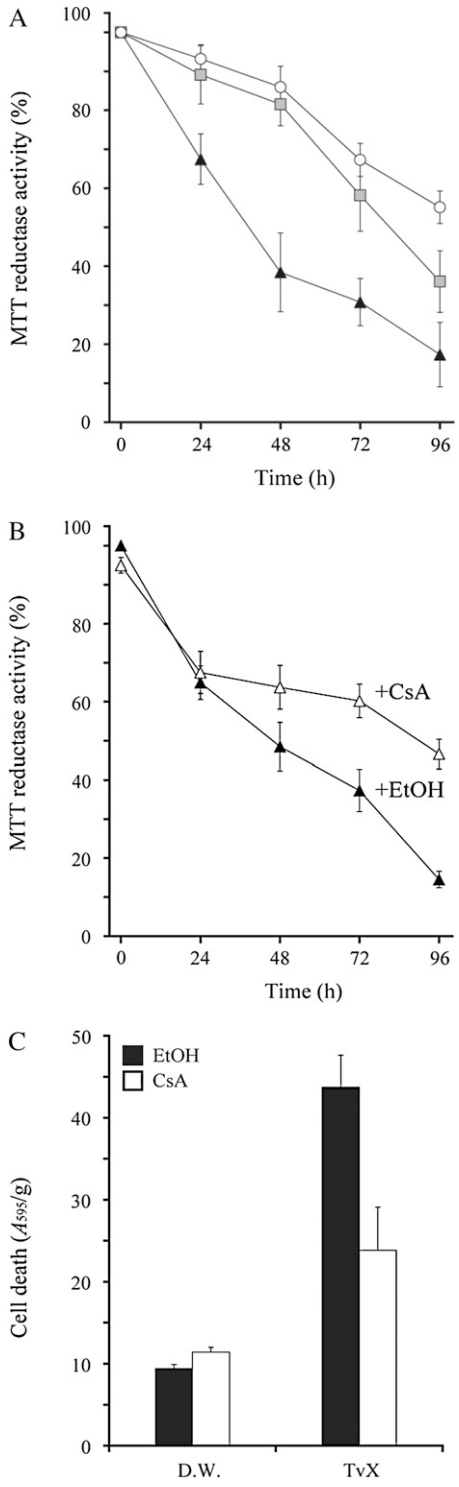

Figure 5. Effects of mitochondrial dysfunction and the suppression of *OsCIPK14/15* on TvX/EIX-induced hypersensitive cell death. A, Effects of the suppression of *OsCIPK14/15* on the TvX/EIX (120 μg mL^{-1})-induced reduction in MTT reductase activity. MTT reductase activity is a putative marker for mitochondrial dysfunction. Black triangles, control line; light gray squares, *RNAi-1*; white circles, *RNAi-2*. B, Effects of a potent inhibitor for mitochondrial permeability transition (CsA) on mitochondrial dysfunction in rice cells treated with the TvX/EIX elicitor (120 μg mL^{-1}). C, Effects of CsA on the TvX/EIX elicitor-induced cell death in rice cells. Rice cells were tested at 72 h after the addition of the TvX/EIX elicitor. CsA (5 μM) or ethanol (EtOH) was added to rice cells 30 min prior to the elicitor treatment. Average values and SE of three independent experiments are shown. Ethanol was used as a control. D.W., Distilled water as a control.

DISCUSSION

This study identified and characterized the two MAMP-induced *CIPK*s, OsCIPK14/15, which interact with Ca^{2+} sensor proteins, OsCBLs. Functional characterization of the *OsCIPK14/15-RNAi* lines as well as overexpressors suggested that the CIPKs are involved in various TvX/EIX-induced layers of defense responses, including hypersensitive cell death, mitochondrial dysfunction, phytoalexin biosynthesis, and PR gene expression.

Biochemical Properties of OsCIPK14/15 and Their Interaction with Rice CBLs

Our results suggest that the FISL/NAF motif in OsCIPK14/15 is an important element to interact with native rice CBLs that have Ca^{2+}-binding activity (Fig. 2, B and F) and that the interaction with OsCBL4 is necessary for cancellation of the autoinhibitory function of OsCIPK14/15 (Fig. 3, B–D). The binding of AtCBL1 to AtCIPK1 is highly dependent on external Ca^{2+} (Shi et al., 1999). The protein kinase activity of AtCIPK24/SOS2 also depends on both AtCBL4/SOS3 and external Ca^{2+} (Halfter et al., 2000). OsCIPK14 and OsCIPK15 may be inactivated by autoinhibition at a resting cytosolic Ca^{2+} level and could be activated upon elicitation by MAMPs through the binding of a Ca^{2+}-bound form of OsCBLs via their FISL/NAF motif. The common machinery for the regulation of CBL-CIPK seems to be highly conserved in a variety of plant species.

Although each CIPK family member has been assumed to interact specifically with a subset of CBLs to transmit Ca^{2+} signals to downstream components, interaction between OsCBLs and OsCIPKs has not yet been reported except for the interaction between OsCBL4 and OsCIPK24 (Martinez-Atienza et al., 2007). We here showed that OsCIPK14 and OsCIPK15 interact with at least five OsCBLs (OsCBL2, OsCBL3, OsCBL4, OsCBL5, and OsCBL6) but not with OsCBL9 in yeast cells (Fig. 2, A–D). Among the OsCBLs, the interaction was strongest with OsCBL4, which was shown to bind Ca^{2+} (Fig. 2F) and to be transcriptionally induced by TvX elicitor (Supplemental Fig. S5). Since overexpression of the mutant form of OsCIPK15 defective in the FISL/NAF motif had no effect on the TvX/EIX-induced hypersensitive cell death (Fig. 8B), some OsCBLs or other unknown factors that interact with OsCIPK15 via the FISL/NAF motif may regulate the activity and localization of OsCIPK14/15 in the MAMP-triggered signal transduction pathway.

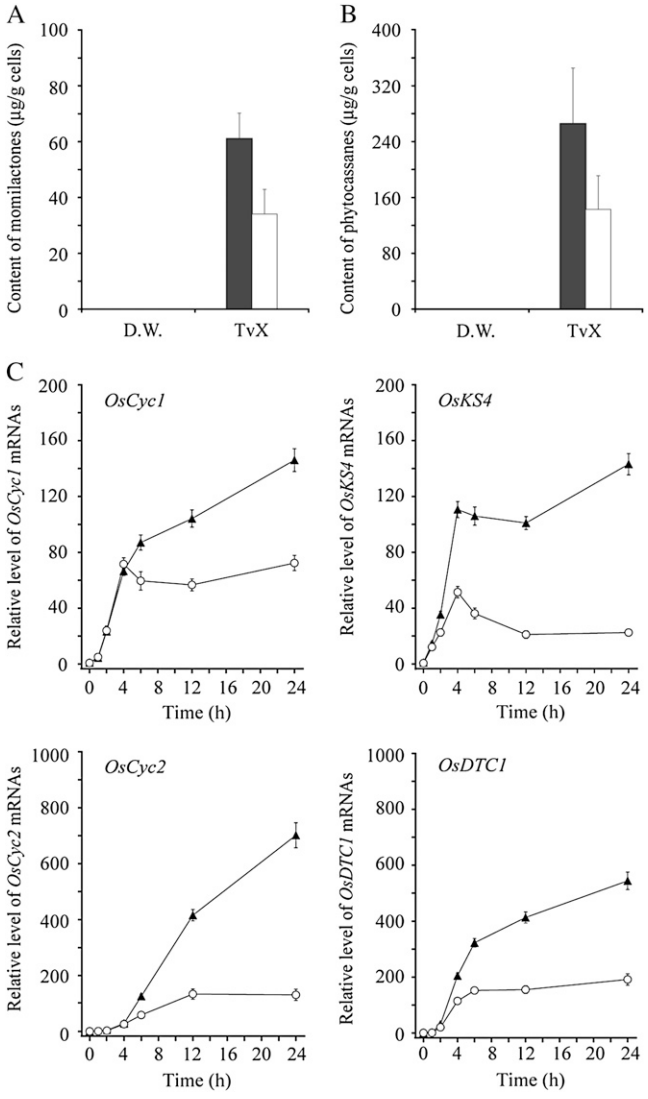

Figure 6. Involvement of OsCIPK14/15 in the regulation of TvX/EIX-induced phytoalexin biosynthesis. A and B, TvX/EIX-induced phytoalexin accumulation in the culture medium. Amounts of momilactones (A) and phytocassanes (B) 72 h after the addition of TvX/EIX (120 μg mL^{-1}) or water were quantified by HPLC as described in "Materials and Methods." Average values and SE of six independent experiments for the control line (black bars) and *RNAi-2* line (white bars) are shown. C, Quantification of the expression levels of the genes involved in biosynthesis of the phytoalexins *OsCyc1*, *OsKS4*, *OsCyc2*, and *OsDTC1* in the control line (black triangles) and *RNAi-2* line (white circles) by real-time quantitative PCR. Total RNA was isolated from the cells harvested at the indicated time points of TvX/EIX treatment (120 μg mL^{-1}). The amount of each mRNA was calculated from the threshold point located in the log-linear range of RT-PCR. The relative level of each gene in control cells at time 0 was standardized as 1. The error bars indicate SD of three experiments. D.W., Distilled water as a control.

The Role of OsCIPK14 and OsCIPK15 in MAMP-Triggered Innate Immune Responses

Phytoalexin production is commonly associated with defense responses in plants. Although MAMP-triggered cytosolic free Ca^{2+} concentration increases have been proposed to be involved in their regulation (Mithöfer et al., 1999; Blume et al., 2000), Ca^{2+}-regulated signaling components still remain mostly unknown. We have shown that TvX/EIX-induced accumulation of momilactones and phytocassanes as well as induction of the cyclase genes, the key enzymes responsible for the biosynthesis of these phytoalexins (Otomo et al., 2004a), are impaired in the *OsCIPK14/15-RNAi* lines (Fig. 6, A and B). These results suggest that OsCIPK14/15 is involved in the regulation of phytoalexin production through transcriptional activation of key enzymes, including diterpene cyclase.

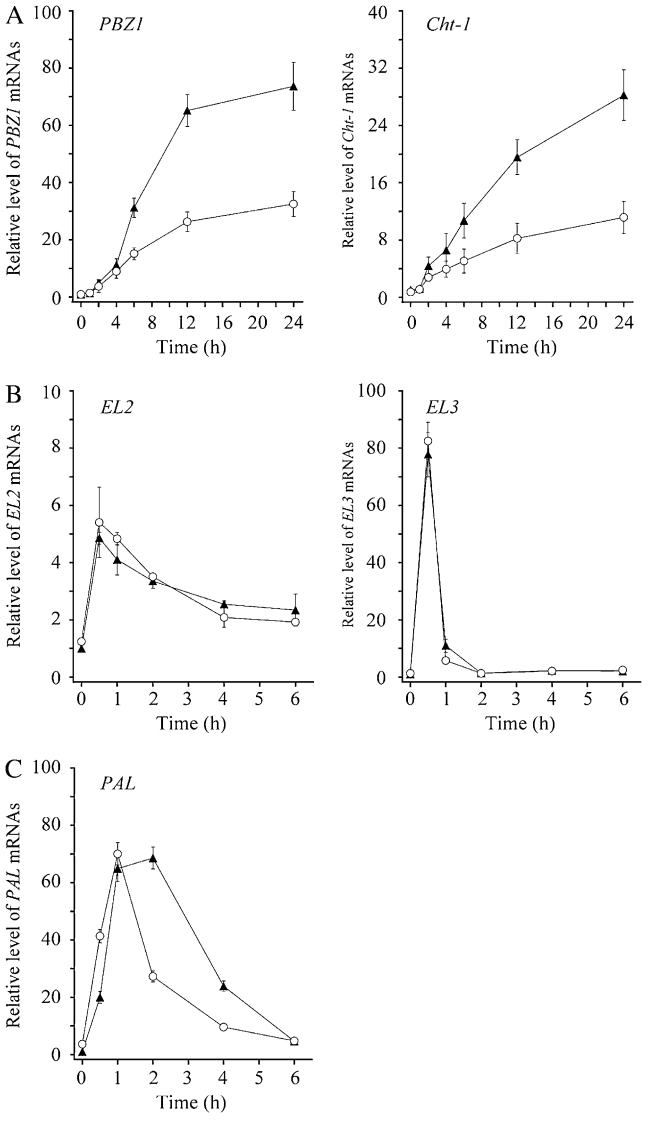

Figure 7. Involvement of OsCIPK14/15 in TvX/EIX-induced PR gene expression. mRNA accumulations of *PBZ1*, *Cht-3*, *EL2*, *EL3*, and *PAL* in the control line (black triangles) and *RNAi-2* line (white circles) are shown. Total RNA was isolated from rice cells harvested at the indicated time points of TvX/EIX treatments (120 μg mL^{-1}). The amount of each mRNA was calculated from the threshold point located in the log-linear range of RT-PCR. The relative level of each gene in control cells at time 0 was standardized as 1. The error bars indicate SD of three experiments.

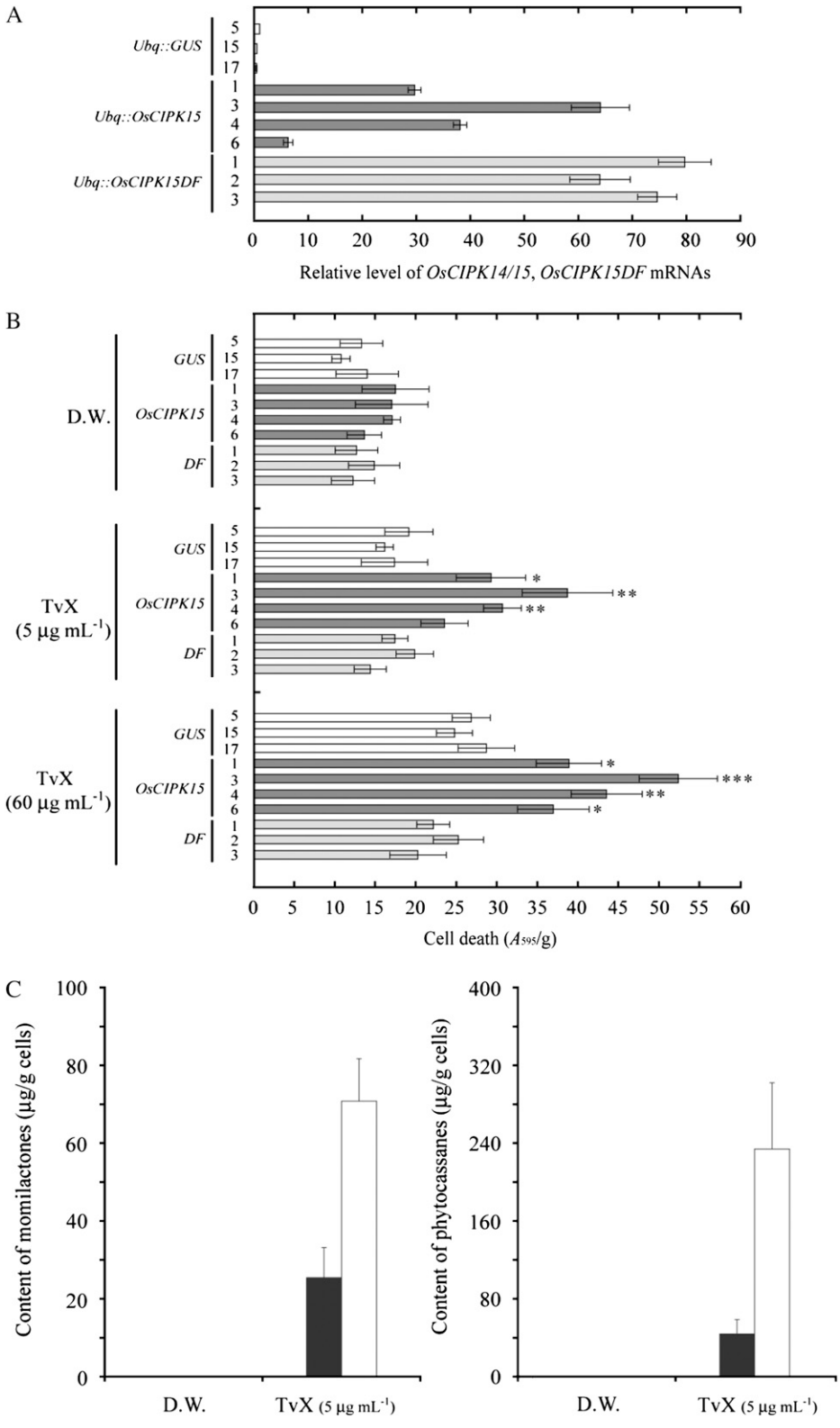

Figure 8. Effects of *OsCIPK15* and *OsCIPK15DF* overexpression on TvX/EIX elicitor-induced hypersensitive cell death and phytoalexin accumulation. A, Quantitative expression level of *OsCIPK14/15* mRNA in both *OsCIPK15* and *OsCIPK15DF* overexpressor lines by real-time quantitative PCR. The amounts of *OsCIPK14/15* mRNAs were calculated from the threshold point located in the log-linear range of RT-PCR. The relative level of the *OsCIPK14/15* mRNAs in the *GUS*-expressing control line (GUS line 5) was standardized as 1. The error bars indicate SD of three experiments. B, TvX/EIX-induced dose-dependent cell death in the *OsCIPK15* and *OsCIPK15DF* overexpressor lines. Rice cells were tested at 24 h after the addition of the TvX/EIX elicitor at various concentrations. Evans blue staining was applied to quantify the level of TvX/EIX-induced cell death. Average values and SE of three independent experiments are shown. * $P < 0.05$, ** $P < 0.01$, *** $P < 0.005$, significant difference as compared with the control line (GUS line 5). C, TvX/EIX-induced phytoalexin accumulation in the culture medium. Amounts of momilactones and phytocassanes 72 h after the addition of the TvX/EIX (5 μg mL^{-1}) or water were quantified by HPLC as described in "Materials and Methods." Average values and SE of three independent experiments for the control line (GUS line 5; black bars) and *OsCIPK15*-overexpressing line (OsCIPK15 line 3; white bars) are shown. D.W., Distilled water as a control.

Expression of *OsCIPK14/15* is also reported to be up-regulated by salt stress, and overexpression of *OsCIPK15* confers improved salt tolerance (Xiang et al., 2007). Since recent studies reveal that alternative CBL/CIPK complexes at different membranes create a dual function in salt stress responses in Arabidopsis (Qiu et al., 2002; Kim et al., 2007; Waadt et al., 2008), OsCBL/OsCIPK14/15 complexes may be involved in multiple defense responses against biotic and abiotic stress. Alternatively, other components that interact

with OsCIPK15 via the FISL/NAF motif may function as a limiting factor for the MAMP-triggered signal transduction pathway.

Increasing evidence suggests the importance of mitochondria in the induction of hypersensitive cell death in defense signaling pathways (Lam et al., 2001; Yao et al., 2004). TvX/EIX-induced cell death (Fig. 5C) and the reduction in putative mitochondrial reductase activity (Fig. 5B) were inhibited by CsA, an inhibitor of mitochondrial permeability transition, suggesting the involvement of mitochondrial dysfunction on TvX/EIX-induced hypersensitive cell death in rice.

TvX/EIX-induced mitochondrial dysfunction as well as hypersensitive cell death requires extracellular Ca^{2+} and a putative Ca^{2+}-permeable channel, OsTPC1 (Kurusu et al., 2005). Our results here indicate that OsCIPK14/15 is also crucial for TvX/EIX-induced mitochondrial dysfunction as well as hypersensitive cell death (Figs. 4, C and D, and 5A), suggesting that OsCIPK14/15 may be involved in transducing MAMP-triggered Ca^{2+} signals to regulate the mitochondria-mediated hypersensitive cell death pathway. OsPDCD5, which is involved in programmed cell death during leaf and root senescence, has been suggested to be phosphorylated by OsCIPK23 (Su et al., 2006). Interestingly, the basal level of the cell death in the *OsCIPK15*-overexpressing lines was slightly higher than in *GUS*-expressing control lines (Fig. 8B). OsCIPK15 may control the activation of cell death regulators. Searches for the in vivo substrates of OsCIPK14 and OsCIPK15 are currently under way to further understand the relationship between Ca^{2+} signaling and the regulation of hypersensitive cell death in innate immunity.

Finally, to test whether OsCIPK14/15 has a role in disease resistance in adult plants, we inoculated the *OsCIPK14/15-RNAi* and *OsCIPK15*-overexpressring plants with the rice blast fungus *Magnaporthe grisea*. Overexpression of *OsCIPK15* and suppression of *OsCIPK14/15* by *RNAi* did not show any significant effect on the growth of an incompatible and a compatible fungus (Supplemental Fig. S7). In adult plants, the contribution of OsCIPK14/15 to resistance against rice blast fungus may be limited. Future infection assays with various kinds of pathogens as well as detailed elucidation of the defense signaling network in the *OsCIPK14/15* mutants would reveal the roles of the CIPKs in vivo in intact plants.

In summary, this study indicates that two CBL-activated protein kinases, OsCIPK14 and OsCIPK15, are involved in the regulation of the defense signaling pathway in rice cultured cells. These findings shed light on our understanding of defense signaling pathways.

MATERIALS AND METHODS

Plant Materials, Cell Cultures, and MAMPs

Surface-sterilized seeds of rice (*Oryza sativa* 'Nipponbare') were germinated on Murashige and Skoog medium (Murashige and Skoog, 1962) containing 0.8% agar and grown for 10 d in a growth chamber under long-day conditions (16 h of light/8 h of darkness, 28°C). Seedlings were transplanted into soil and grown in a greenhouse (16 h of light/8 h of darkness, 28°C, 60% humidity). To generate cultured cells, including the *OsCIPK14/15-RNAi* lines, seeds were placed onto callus-inducing medium. The calli were suspension cultured at 25°C in a liquid L medium (Kuchitsu et al., 1993) containing 2,4-dichlorophenoxyacetic acid (0.5 mg L^{-1}) and subcultured in fresh medium every 7 d. Cells at 5 d after subculture were used for experiments with MAMPs. TvX/EIX was obtained from Sigma. *N*-Acetylchitooligosaccharide was kindly provided by Prof. Naoto Shibuya (Meiji University).

Isolation of *OsCIPK14* and *OsCIPK15* cDNA

The estimated coding region of *OsCIPK14* and *OsCIPK15* was amplified by PCR using two primers each, OsCIPK14FW1, 5′-ATGGAGAGTAGAGGGAAGATA-3′; OsCIPK14RV1, 5′-CTATTCATCTCCATGCCAGGC-3′; OsCIPK15FW1, 5′-ATGGAGAGTAGAGGGAAGATT-3′; OsCIPK15RV1, 5′-CTATTCATCTCCATGC-3′. Total RNA was isolated from leaves of rice with Trizol (Invitrogen) in accordance with the manufacturer's protocol and quantified spectrophotometrically. First-strand cDNA was synthesized from 3 μg of total RNA with the oligo(dT) primer and reverse transcriptase (Invitrogen). To obtain full-length cDNAs for *OsCIPK14* and *OsCIPK15* and to define the open reading frame, 3′-RACE-PCR and 5′-RACE-PCR were performed with a 3′-full RACE core kit (Takara) and a 5′-RACE system (Invitrogen) in accordance with the manufacturer's protocol.

Plasmid Construction

The coding regions of OsCIPK14 and OsCIPK15 and OsCBL4 and OsCBL9 were amplified by PCR with primers harboring additional sequence (the CACC sequences are underlined) for use with the Gateway system, subcloned into the pENTR/D-TOPO cloning vector (Invitrogen) to yield entry vectors, and cloned into pDEST15 vector (Invitrogen) using LR clonase reaction (Invitrogen). The PCR primers were OsCIPK14FW2, 5′-CACCATGGAGAGTAGAGGGAAGATA-3′; OsCIPK14RV2, 5′-CTATTCATCTCCATGCCAGGCCAAG-3′; OsCIPK15FW2, 5′-CACCATGGAGAGTAGAGGGAAGATT-3′; OsCIPK15RV2, 5′-CTAGGCCAAGACAATGTCCTTCAGA-3′; OsCBL4FW2, 5′-CACCATGGGATGCGCGTCGTCGAAG-3′; OsCBL4RV2, 5′-TCAGTCATGGGCTTCTGAATGCATT-3′; OsCBL9FW2, 5′-CACCATGGAGTCGGGCTACGGCTT-3′; and OsCBL9RV2, 5′-CTAAAACAATCCAAAGGGAG-3′.

To make the deletion mutants (OsCIPK14DF and OsCIPK15DF), the following primer pairs were used for PCR amplification: the forward primers OsCIPK14DF-FW1, 5′-GGATCCATGGAGAGTAGAGGGAA-3′; OsCIPK15DF-FW1, 5′-GGATCCATGGAGAGTAGAGGGAA-3′ (the *Bam*HI site is underlined in each primer); OsCIPK14DF-FW2, 5′-ATTGTAAAGGAATGGAGAAATGAGG-3′; OsCIPK15DF-FW2, 5′-ATTGTAAAGGAATGGAGAAATGAGG-3′ and the reverse primers OsCIPK14DF-RV1, 5′-TAAGTTTGTCACTGACATGGGCTTC-3′; OsCIPK15DF-RV1, 5′-TAAGTTTGTCACTGACATGGGCTTC-3′; OsCIPK14DF-RV2, 5′-TCTAGACTATTCATCTCCATGCC-3′; OsCIPK15DF-RV2, 5′-TCTAGACTAGGCCAAGACAATGT-3′ (the *Xba*I site is underlined in each primer). First-round PCR products were amplified with OsCIPK14DF-FW1 and OsCIPK14DF-RV1, OsCIPK15DF-FW1 and OsCIPK15DF-RV1, OsCIPK14DF-FW2 and OsCIPK14DF-RV2, and OsCIPK15DF-FW2 and OsCIPK15DF-RV2. Each PCR fragment was subcloned into pBluescript II SK+ (Stratagene) between the *Bam*HI and *Xba*I sites. These vector constructs were used as templates for amplification using OsCIPK14FW2 and OsCIPK14RV2 and OsCIPK15FW2 and OsCIPK15RV2, subcloned into the pENTR/D-TOPO cloning vector, and then cloned into a pDEST15 vector using the LR clonase reaction.

The coding regions of *OsCIPK14* and *OsCIPK15* were amplified by PCR with primers harboring restriction sites and cloned in frame into the pGBKT7 vector (Clontech). The following PCR primers were used: OsCIPK14FW3, 5′-GGATCCGTATGGAGAGTAGAGGGAA-3′ (the *Bam*HI site is underlined); OsCIPK14RV3, 5′-CTGCAGTATTCATCTCCATG-3′ (the *Pst*I site is underlined); OsCIPK15FW3, 5′-GGATCCGTATGGAGAGTAGAGGGAA-3′ (the *Bam*HI site is underlined); and OsCIPK15RV3, 5′-CTGCAGTAGGCCAAGACAAT-3′ (the *Pst*I site is underlined). The pBluescriptII-OsCIPK14DF and -OsCIPK15DF constructs were used as PCR templates to make pGBKT7-OsCIPK14DF and -OsCIPK15DF constructs, respectively. The coding region of *OsCBL2*, *OsCBL3*, *OsCBL4*, *OsCBL5*, *OsCBL6*, and *OsCBL9* was amplified by PCR with primers harboring restriction sites and cloned in frame into the

pGADT7 vector (Clontech). The following PCR primers were used: OsCBL2FW3, 5′-GAATTCATGGTGCAGTGTCTCGAC-3′ (the *Eco*RI site is underlined); OsCBL2RV3, 5′-CCCGGGTCAGGTGTCATCGACC-3′ (the *Sma*I site is underlined); OsCBL3FW3, 5′-GAATTCATGTTGCAGTGTCTGGAG-3′ (the *Eco*RI site is underlined); OsCBL3RV3, 5′-CCCGGGTCAAGTATCGTC-GACT-3′ (the *Sma*I site is underlined); OsCBL4FW3, 5′-GAATTCATGGGA-TGCGCGTCGTCG-3′ (the *Eco*RI site is underlined); OsCBL4RV3, 5′-CCCGGG-TCAGTCATGGGCTTCT-3′ (the *Sma*I site is underlined); OsCBL5FW3, 5′-CCCGGGGATGATGGGCTGTCTA-3′ (the *Sma*I site is underlined); OsCBL5RV3, 5′-GAGCTCTTAGGCAACCATGTCTGC-3′ (the *Sac*I site is underlined); OsCBL6FW3, 5′-CCCGGGGATGGTGGATTCCTCG-3′ (the *Sma*I site is underlined); OsCBL6RV3, 5′-GAGCTCTCATGCGTCCTCAACCTG-3′ (the *Sac*I site is underlined); OsCBL9FW3, 5′-GAATTCATGGTGGGGCCAGGCCTG-3′ (the *Eco*RI site is underlined); OsCBL9RV3, 5′-CCCGGGCTAAAACAATCCA-AAG-3′ (the *Sma*I site is underlined).

RNA Isolation, RT-PCR, and Northern-Blot Analyses

Total RNA was isolated from rice cells using Trizol reagent in accordance with the manufacturer's protocol and quantified using a spectrophotometer. First-strand cDNA was synthesized from 3 μg of total RNA with an oligo(dT) primer and reverse transcriptase. PCR amplification was performed with an initial denaturation at 95°C for 3 min followed by the indicated number of cycles of incubations at 94°C for 30 s, 55°C for 90 s, and 72°C for 1 min using specific primers (Supplemental Table S1). *Ubiquitin* was used as a quantitative control. Aliquots of individual PCR products were resolved by agarose gel electrophoresis and visualized using ethidium bromide staining by exposure to UV light.

Because *OsCIPK14* and *OsCIPK15* have no introns, we confirmed that the PCR products from RT-PCR were derived from cDNA and not from genomic DNA by performing control experiments comparing samples with or without reverse transcriptase treatment. We only detected PCR products for *OsCIPK14* and *OsCIPK15* in the presence of reverse transcriptase (Supplemental Fig. S4), indicating that the PCR products were derived from cDNA.

For Northern-blot analyses, 20 μg of total RNA was resolved by electrophoresis on a 1% agarose gel containing 5.5% formaldehyde and transferred to a nylon membrane filter (Hybond-N+; GE Healthcare Bio-Sciences). ^{32}P-labeled probes were obtained as gene-specific 0.4-kb fragments from the 3′ end of the *OsCIPK14* gene, including 3′ untranslated sequences. Hybridization was carried out at 42°C in a solution that contained sodium phosphate buffer (pH 7.2), 7% SDS, and 20 μg mL^{-1} denatured salmon sperm DNA, and stringent washing was performed at 55°C in 2× SSC and 0.1% SDS. The signals were analyzed quantitatively using Typhoon 9210 (GE Healthcare Bio-Sciences) and ImageQuant software.

Real-Time RT-PCR Quantification

First-strand cDNA was synthesized from 3 μg of total RNA with an oligo (dT) primer and reverse transcriptase. Real-time PCR was performed using an ABI PRISM 7300 sequence detection system (Applied Biosystems) with SYBR Green real-time PCR Master Mix (Toyobo) and the gene-specific primers (Supplemental Table S1). Relative mRNA abundances were calculated using the standard curve method and normalized to the corresponding *OsActin1* gene levels. Standard samples of known template amounts were used to quantify the PCR products.

Phytoalexin Measurements

The amounts of induced diterpenoid phytoalexins (momilactones and phytocassanes) in the culture medium were analyzed by HPLC. An Agilent 1100 separation module (Agilent Technologies) equipped with a Pegasil C18 column (150 mm × 2.1 mm in diameter; Senshu Scientific) was used for the HPLC analysis. For diterpenoid phytoalexins, elution was conducted in 70% aqueous acetonitrile containing 0.1% acetic acid at a flow rate of 0.2 mL min^{-1}. The respective authentic samples of diterpenoid phytoalexins were dissolved in 79% aqueous ethanol containing 7% aqueous acetonitrile and 0.01% acetic acid, which was used as a standard solution. For the selection of diagnostic precursor-to-product ion transitions, the standard solutions were directly infused at a flow rate of 5 mL min^{-1} into a quadrupole tandem mass spectrometer (API-3000; Applied Biosystems Instruments) fitted with an electrospray ion source. All diterpenoid phytoalexins were analyzed in positive-ion mode. Nitrogen was used as the collision gas. The electrospray capillary was set at 3.0 kV, and the source temperature was 400°C. Other parameters were optimized using spectrometer software (Applied Biosystems Instruments). The diterpenoid phytoalexin levels were determined with combinations of mass-to-charge ratio (*m/z*) 315/271 (precursor/product ions) for momilactone A, *m/z* 331/269 for momilactone B, *m/z* 317/299 for phytocassanes A, D, and E, and *m/z* 319/301 for phytocassane C in the multiple reaction monitoring mode.

Expression and Purification of OsCIPK and OsCBL Proteins

The plasmids pDEST15-*OsCIPK14*, -*OsCIPK15*, -*OsCIPK14DF*, and -*OsCIPK15DF* and pDEST15-*OsCBL4* and -*OsCBL9* were transformed separately into *Escherichia coli* BL21-AI (Invitrogen). Fresh cultures of *E. coli* carrying the foreign genes were cultured at 37°C until the A_{600} of the culture medium reached 0.5. To induce GST fusion protein expression, Ara was added to a final concentration of 0.2%. After 12-h induction of the cultures at 20°C, the cells were harvested by centrifugation, resuspended in cold phosphate-buffered saline (PBS) buffer, and lysed by the freeze-thaw method in accordance with the supplier's instructions. The cell lysate was centrifuged at 10,000*g* for 10 min at 4°C, and the supernatant was applied onto a glutathione-Sepharose 4B column (GE Healthcare Bio-Sciences). After washing the column with PBS buffer, GST fusion proteins were eluted with 5 mM glutathione in PBS buffer and used for both the kinase activity and Ca^{2+} mobility shift assays.

Protein Kinase Assay

For autophosphorylation activity and cofactor dependence of OsCIPK14/15, aliquots of GST-OsCIPK14/15 fusion proteins (100 ng) were incubated in kinase assay buffer (10 μCi of [γ-^{32}P]ATP, 20 mM Tris-HCl, pH 8.0, 1 mM dithiothreitol [DTT], and either 5 mM $MgCl_2$, $MnCl_2$, $CaCl_2$, or EDTA) for 10 min at 37°C. For autophosphorylation activity of OsCIPK14/15 in the presence of OsCBLs, aliquots of GST-OsCIPK14/15 or GST-OsCIPK14DF/15DF fusion proteins in the presence or absence of GST-OsCBL4 and GST-OsCBL9 fusion proteins were incubated in the kinase assay buffer (10 μCi of [γ-^{32}P] ATP, 20 mM Tris-HCl, pH 8.0, 1 mM DTT, and 5 mM $MnCl_2$, with or without 1 mM $CaCl_2$) for 10 min at 37°C. The reaction was stopped by the addition of 4× SDS sample buffer, boiled immediately for 5 min, and analyzed by 7.5% SDS-PAGE. Gels were stained with Coomassie Brilliant Blue and dried, and their signals were obtained quantitatively using Typhoon 9210 with ImageQuant software and normalized by the intensity of Coomassie Brilliant Blue staining with the corresponding protein.

Yeast Two-Hybrid Analyses

A Matchmaker Gal4-based Two-Hybrid System 3 was used as described by the manufacturer (Clontech). Yeast strain AH109 was cotransformed with each pBD-*OsCIPK* (*OsCIPK14*, *OsCIPK15*, *OsCIPK14DF*, and *OsCIPK15DF*) and with each pAD-*OsCBL* (*OsCBL2*, *OsCBL3*, *OsCBL4*, *OsCBL5*, *OsCBL6*, and *OsCBL9*) by the lithium acetate method. Cotransformants were first screened on synthetic medium lacking Leu and Trp (SD/−Leu/−Trp). The yeast cells were then streaked onto the medium lacking Leu, Trp, and His (SD/−Leu/−Trp/−His) containing X-α-Gal (40 μg mL^{-1}).

For quantitative assays, yeast strain Y187 was cotransformed with each pBD-*OsCIPK* (*OsCIPK14*, *OsCIPK15*, *OsCIPK14DF*, and *OsCIPK15DF*) and each pAD-*OsCBL* (*OsCBL2*, *OsCBL3*, *OsCBL4*, *OsCBL5*, *OsCBL6*, and *OsCBL9*) by the lithium acetate method. Assays of β-galactosidase activity were performed in triplicate using chlorophenol red-β-D-galactopyranoside as the substrate in accordance with the manufacturer's protocol (Clontech). β-Galactosidase activity was calculated using the following equation: units of β-galactosidase activity = $1{,}000 \times A_{578}/(T \times V \times A_{600})$, where V is the volume of the culture (mL), T is the reaction time (min), and A_{600} is the optical density of the yeast cells at 600 nm.

Transgenic Rice Cells

For generating the RNA-silencing-triggered inverted repeat constructs, the region (340 bp of the 3′ untranslated region of *OsCIPK14*) was amplified using RNAiFW, 5′-CACCAATGGTGTAGTGAAGATGCAA-3′ and RNAiRV, 5′-CTCCAGATACAAAAACATAGATGCT-3′ as the specific primers, subcloned into the pENTR/D-TOPO cloning vector, and then cloned into the Ti-based

RNAi vector pANDA (Miki and Shimamoto, 2004) using the LR clonase reaction. The construct was introduced into rice calli by means of *Agrobacterium tumefaciens*-mediated transformation in accordance with the method of Tanaka et al. (2001). Transformed calli were screened by hygromycin selection (50 μg mL^{-1}), followed by regeneration of transgenic plants. Transgenic cell lines derived from T2 plants were used for various analyses.

To overexpress *OsCIPK15*, *OsCIPK15DF*, and *GUS* cDNAs, the sequences were cloned into the Ti-based vector pPZP2H-lac (Fuse et al., 2001) downstream of the maize (*Zea mays*) ubiquitin promoter, and *Agrobacterium*-mediated transformation of rice calli was performed. Transformed calli were screened by hygromycin selection (50 μg mL^{-1}), followed by regeneration of transgenic plants.

Cell Death Assay with Evans Blue

An aliquot of the cell suspension (50 mg fresh weight in 0.5 mL) was incubated with 0.05% Evans blue (Sigma) for 10 min and washed to remove unabsorbed dye. The selective staining of dead cells with Evans blue depends on extrusion of the dye from living cells via an intact plasma membrane (Turner and Novacky, 1974). Dye that had been absorbed by dead cells was extracted with 50% methanol plus 1% SDS for 1 h at 60°C and quantified by A_{595}.

MTT Reductase Assay

An aliquot of the cell suspension (50 mg fresh weight in 0.5 mL) was incubated with 0.2 mL of 12 mM MTT solution (Dojindo) for 0.5 h at 28°C. The supernatant was removed by centrifugation, and 1 mL of acidic isopropanol (40 mM HCl) was added to the stained cells, followed by incubation at 60°C for 15 min to elute the dye from the cells. A_{595} was determined to measure the reductase activity.

Statistical Analysis

Statistical significance was determined using an unpaired Student's *t* test with $P < 0.05$ required for significance.

Sequence data from this article can be found in the GenBank/EMBL data libraries under accession numbers AB264036 and AB264037.

Supplemental Data

The following materials are available in the online version of this article.

Supplemental Figure S1. Comparative expression analysis of several *OsCIPK*s in response to MAMPs.

Supplemental Figure S2. Alignment of the predicted amino acid sequences of OsCIPK14, OsCIPK15, and SOS2.

Supplemental Figure S3. Expression of *OsCIPK14/15* genes in rice.

Supplemental Figure S4. Confirmation of PCR products of *OsCIPK14* and *OsCIPK15* with or without reverse transcriptase treatment.

Supplemental Figure S5. Induction of *OsCBL4* genes in response to MAMPs.

Supplemental Figure S6. Schematic diagrams of OsCIPK14 and OsCIPK15 mutants (OsCIPK14/15DF).

Supplemental Figure S7. Effects of the expression levels of *OsCIPK14/15* on disease resistance against rice blast fungus.

Supplemental Table S1. Sequences of RT-PCR primers used in this experiment.

Supplemental Materials and Methods S1. Quantification of *Magnaporthe grisea* growth in rice leaves.

ACKNOWLEDGMENTS

We thank Mr. Kazuki Iwabata and Dr. Hidetaka Kaya for helpful technical suggestions and discussion, Mr. Yohei Iwasaki for technical assistance, Drs. Daisuke Miki and Ko Shimamoto for the *RNAi* plasmid (pANDA vector), Dr. Naoto Shibuya for the gift of *N*-acetylchitoheptaose, and Drs. Morifumi Hasegawa and Osamu Kodama for the gift of momilactones.

Received December 9, 2009; accepted March 29, 2010; published March 31, 2010.

LITERATURE CITED

Albrecht V, Ritz O, Linder S, Harter K, Kudla J (2001) The NAF domain defines a novel protein-protein interaction module conserved in Ca^{2+}-regulated kinases. EMBO J **20:** 1051–1063

Batistic O, Kudla J (2004) Integration and channeling of calcium signaling through the CBL calcium sensor/CIPK protein kinase network. Planta **219:** 915–924

Batistic O, Kudla J (2009) Plant calcineurin B-like proteins and their interacting protein kinases. Biochim Biophys Acta **1793:** 985–992

Blume B, Nürnberger T, Nass N, Scheel D (2000) Receptor-mediated increase in cytoplasmic free calcium required for activation of pathogen defense in parsley. Plant Cell **12:** 1425–1440

Cho EM, Okada A, Kenmoku H, Otomo K, Toyomasu T, Mitsuhashi W, Sassa T, Yajima A, Yabuta G, Mori K, et al (2004) Molecular cloning and characterization of a cDNA encoding *ent*-cassa-12,15-dienesynthase, a putative diterpenoid phytoalexin biosynthetic enzyme, from suspension-cultured rice cells treated with a chitin elicitor. Plant J **37:** 1–8

Fuse T, Sasaki T, Yano M (2001) Ti-plasmid vectors useful for functional analysis of rice genes. Plant Biotechnol **18:** 219–222

Gong D, Gong Z, Guo Y, Chen X, Zhu JK (2002a) Biochemical and functional characterization of PKS11, a novel *Arabidopsis* protein kinase. J Biol Chem **277:** 28340–28350

Gong D, Gong Z, Guo Y, Zhu JK (2002b) Expression, activation, and biochemical properties of a novel Arabidopsis protein kinase. Plant Physiol **129:** 225–234

Greenberg JT, Yao N (2004) The role and regulation of programmed cell death in plant-pathogen interactions. Cell Microbiol **6:** 201–211

Guo Y, Halfter U, Ishitani M, Zhu JK (2001) Molecular characterization of functional domains in the protein kinase SOS2 that is required for plant salt tolerance. Plant Cell **13:** 1383–1400

Halfter U, Ishitani M, Zhu JK (2000) The *Arabidopsis* SOS2 protein kinase physically interacts with and is activated by the calcium-binding protein SOS3. Proc Natl Acad Sci USA **97:** 3735–3740

Harmon AC, Gribskov M, Harper JF (2000) CDPKs—a kinase for every Ca^{2+} signal? Trends Plant Sci **5:** 154–159

Heo WD, Lee SH, Kim MC, Kim JC, Chung WS, Chun HJ, Lee KJ, Park CY, Park HC, Choi JY, et al (1999) Involvement of specific calmodulin isoforms in salicylic acid-independent activation of plant disease resistance responses. Proc Natl Acad Sci USA **96:** 766–771

Hwang YS, Bethke PC, Cheong YH, Chang HS, Zhu T, Jones RL (2005) A gibberellin-regulated calcineurin B in rice localizes to the tonoplast and is implicated in vacuole function. Plant Physiol **138:** 1347–1358

Ikegawa H, Yamamoto Y, Matsumoto H (1998) Cell death caused by a combination of aluminum and iron in cultured tobacco cells. Physiol Plant **104:** 474–478

Kadota Y, Goh T, Tomatsu H, Tamauchi R, Higashi K, Muto S, Kuchitsu K (2004a) Cryptogein-induced initial events in tobacco BY-2 cells: pharmacological characterization of molecular relationship among cytosolic Ca^{2+} transients, anion efflux and production of reactive oxygen species. Plant Cell Physiol **45:** 160–170

Kadota Y, Watanabe T, Fujii S, Higashi K, Sano T, Nagata T, Hasezawa S, Kuchitsu K (2004b) Crosstalk between elicitor-induced cell death and cell cycle regulation in tobacco BY-2 cells. Plant J **40:** 131–142

Kaku H, Nishizawa Y, Ishii-Minami N, Akimoto-Tomiyama C, Dohmae N, Takio K, Minami E, Shibuya N (2006) Plant cells recognize chitin fragments for defense signaling through a plasma membrane receptor. Proc Natl Acad Sci USA **103:** 11086–11091

Karita E, Yamakawa H, Mitsuhara I, Kuchitsu K, Ohashi Y (2004) Three types of tobacco calmodulins characteristically activate plant NAD kinase at different Ca^{2+} concentrations and pHs. Plant Cell Physiol **45:** 1371–1379

Kikuyama M, Kuchitsu K, Shibuya N (1997) Membrane depolarization induced by *N*-acetylchitooligosaccharide elicitor in suspension-cultured rice cells. Plant Cell Physiol **38:** 902–909

Kim BG, Waadt R, Cheong YH, Pandey GK, Dominguez-Solis JR, Schultke S, Lee SC, Kudla J, Luan S (2007) The calcium sensor CBL10 mediates salt tolerance by regulating ion homeostasis in *Arabidopsis*. Plant J **52:** 473–484

Kim KN, Cheong YH, Grant JJ, Pandey GK, Luan S (2003a) CIPK3, a calcium sensor-associated protein kinase that regulates abscisic acid and cold signal transduction in *Arabidopsis*. Plant Cell **15:** 411–423

Kim KN, Lee JS, Han H, Choi SA, Go SJ, Yoon IS (2003b) Isolation and characterization of a novel rice Ca^{2+}-regulated protein kinase gene involved in responses to diverse signals including cold, light, cytokinins, sugars and salts. Plant Mol Biol **52:** 1191–1202

Kobayashi M, Ohura I, Kawakita K, Yokota N, Fujiwara M, Shimamoto K, Doke N, Yoshioka H (2007) Calcium-dependent protein kinases regulate the production of reactive oxygen species by potato NADPH oxidase. Plant Cell **19:** 1065–1080

Koga J, Ogawa N, Yamauchi T, Kikuchi M, Ogasawara N, Shimura M (1997) Functional moiety for the antifungal activity of phytocassane E, a diterpene phytoalexin from rice. Phytochemistry **44:** 249–253

Koga J, Shimura M, Oshima K, Ogawa N, Yamauchi T, Ogasawara N (1995) Phytocassanes A, B, C and D, novel diterpene phytoalexins from rice, *Oryza sativa* L. Tetrahedron **51:** 7907–7918

Kolukisaoglu U, Weinl S, Blazevic D, Batistic O, Kudla J (2004) Calcium sensors and their interacting protein kinases: genomics of the Arabidopsis and rice CBL-CIPK signaling networks. Plant Physiol **134:** 43–58

Kuchitsu K, Kikuyama M, Shibuya N (1993) *N*-Acetylchitooligosaccharides, biotic elicitors for phytoalexin production, induce transient membrane depolarization in suspension-cultured rice cells. Protoplasma **174:** 79–81

Kuchitsu K, Kosaka H, Shiga T, Shibuya N (1995) EPR evidence for generation of hydroxyl radical triggered by *N*-acetylchitooligosaccharide elicitor and a protein phosphatase inhibitor in suspension-cultured rice cells. Protoplasma **188:** 138–142

Kuchitsu K, Yazaki Y, Sakano K, Shibuya N (1997) Transient cytoplasmic pH change and ion fluxes through the plasma membrane in suspension-cultured rice cells triggered by *N*-acetylchitooligosaccharide elicitor. Plant Cell Physiol **38:** 1012–1018

Kudla J, Xu Q, Harter K, Gruissem W, Luan S (1999) Genes for calcineurin B-like proteins in *Arabidopsis* are differentially regulated by stress signals. Proc Natl Acad Sci USA **96:** 4718–4723

Kurusu T, Yagala T, Miyao A, Hirochika H, Kuchitsu K (2005) Identification of a putative voltage-gated Ca^{2+} channel as a key regulator of elicitor-induced hypersensitive cell death and mitogen-activated protein kinase activation in rice. Plant J **42:** 798–809

Lam E, Kato N, Lawton M (2001) Programmed cell death, mitochondria and the plant hypersensitive response. Nature **411:** 848–853

Lecourieux D, Mazars C, Pauly N, Ranjeva R, Pugin A (2002) Analysis and effects of cytosolic free calcium increases in response to elicitors in *Nicotiana plumbaginifolia* cells. Plant Cell **14:** 2627–2641

Lee SC, Lan WZ, Kim BG, Li L, Cheong YH, Pandy GK, Lu G, Buchanan BB, Luan S (2007) A protein phosphorylation/dephosphorylation network regulates a plant potassium channel. Proc Natl Acad Sci USA **104:** 15959–15964

Li L, Kim BG, Cheong YH, Pandy GK, Luan S (2006) A Ca^{2+} signaling pathway regulates a K^+ channel for low-K response in *Arabidopsis*. Proc Natl Acad Sci USA **103:** 12625–12630

Liu J, Ishitani M, Halfter U, Kim CS, Zhu JK (2000) The *Arabidopsis thaliana* SOS2 gene encodes a protein kinase that is required for salt tolerance. Proc Natl Acad Sci USA **97:** 3730–3734

Liu J, Zhu JK (1998) A calcium sensor homolog required for plant salt tolerance. Science **280:** 1943–1945

Luan S (2009) The CBL-CIPK network in plant calcium signaling. Trends Plant Sci **14:** 37–42

Luan S, Kudla J, Rodriguez-Concepcion M, Yalovsky S, Gruissem W (2002) Calmodulins and calcineurin B-like proteins: calcium sensors for specific signal response coupling in plants. Plant Cell (Suppl) **14:** S389–S400

Ludwig AA, Saitoh H, Felix G, Freymark G, Miersch O, Wasternack C, Boller T, Jones JD, Romeis T (2005) Ethylene-mediated cross-talk between calcium-dependent protein kinase and MAPK signaling controls stress responses in plants. Proc Natl Acad Sci USA **102:** 10736–10741

Mahajan S, Sopory SK, Tuteja N (2006) Cloning and characterization of CBL-CIPK signalling components from a legume (*Pisum sativum*). FEBS J **273:** 907–925

Marchetti P, Hirsch T, Zamzami N, Castedo M, Decaudin D, Susin SA, Masse B, Kroemer G (1996) Mitochondrial permeability transition triggers lymphocyte apoptosis. J Immunol **157:** 4830–4836

Martinez-Atienza J, Jiang X, Garciadeblas B, Mendoza I, Zhu JK, Pardo JM, Quintero FJ (2007) Conservation of the salt overly sensitive pathway in rice. Plant Physiol **143:** 1001–1012

Midoh N, Iwata M (1996) Cloning and characterization of a probenazole-inducible gene for an intracellular pathogenesis-related protein in rice. Plant Cell Physiol **37:** 9–18

Miki D, Shimamoto K (2004) Simple RNAi vectors for stable and transient suppression of gene function in rice. Plant Cell Physiol **45:** 490–495

Minami E, Kuchitsu K, He DY, Kouchi H, Midoh N, Ohtsuki Y, Shibuya N (1996) Two novel genes rapidly and transiently activated in suspension-cultured rice cells by treatment with *N*-acetylchitoheptaose, a biotic elicitor for phytoalexin production. Plant Cell Physiol **37:** 563–567

Mithöfer A, Ebel J, Bhagwat AA, Boller T, Neuhaus-Url G (1999) Transgenic aequorin monitors cytosolic calcium transients in soybean cells challenged with β-glucan or chitin elicitors. Planta **207:** 566–574

Miya A, Albert P, Shinya T, Desaki Y, Ichimura K, Shirasu K, Narusaka Y, Kawakami N, Kaku H, Shibuya N (2007) CERK1, a LysM receptor kinase, is essential for chitin elicitor signaling in *Arabidopsis*. Proc Natl Acad Sci USA **104:** 19613–19618

Murashige T, Skoog F (1962) A revised medium for rapid growth and bioassays with tobacco tissue cultures. Physiol Plant **15:** 473–497

Nishizawa Y, Kawakami A, Hibi T, He DY, Shibuya N, Minami E (1999) Regulation of the chitinase gene expression in suspension-cultured rice cells by *N*-acetylchitooligosaccharides: differences in the signal transduction pathways leading to the activation of elicitor-responsive genes. Plant Mol Biol **39:** 907–914

Nürnberger T, Scheel D (2001) Signal transmission in the plant immune response. Trends Plant Sci **6:** 372–379

Ogasawara Y, Kaya H, Hiraoka G, Yumoto F, Kimura S, Kadota Y, Hishinuma H, Senzaki E, Yamagoe S, Nagata K, et al (2008) Synergistic activation of the Arabidopsis NADPH oxidase AtrbohD by Ca^{2+} and phosphorylation. J Biol Chem **283:** 8885–8892

Otomo K, Kanno Y, Motegi A, Kenmoku H, Yamane H, Mitsuhashi W, Oikawa H, Toshima H, Itoh H, Matsuoka M, et al (2004a) Diterpene cyclases responsible for the biosynthesis of phytoalexins, momilactones A, B, and oryzalexins A-F in rice. Biosci Biotechnol Biochem **68:** 2001–2006

Otomo K, Kenmoku H, Oikawa H, König WA, Toshima H, Mitsuhashi W, Yamane H, Sassa T, Toyomasu T (2004b) Biological functions of *ent*- and *syn*-copalyl diphosphate synthases in rice: key enzymes for the branch point of gibberellin and phytoalexin biosynthesis. Plant J **39:** 886–893

Pugin A, Frachisse JM, Tavernier E, Bligny R, Gout E, Douce R, Guern J (1997) Early events induced by the elicitor cryptogein in tobacco cells: involvement of a plasma membrane NADPH oxidase and activation of glycolysis and the pentose phosphate pathway. Plant Cell **9:** 2077–2091

Qiu QS, Guo Y, Dietrich MA, Schumaker KS, Zhu JK (2002) Regulation of SOS1, a plasma membrane Na^+/H^+ exchanger in *Arabidopsis thaliana*, by SOS2 and SOS3. Proc Natl Acad Sci USA **99:** 8436–8441

Reddy AS (2001) Calcium: silver bullet in signaling. Plant Sci **160:** 381–404

Romeis T, Ludwig AA, Martin R, Jones JD (2001) Calcium-dependent protein kinases play an essential role in a plant defence response. EMBO J **20:** 5556–5567

Romeis T, Piedras P, Jones JD (2000) Resistance gene-dependent activation of a calcium-dependent protein kinase in the plant defense response. Plant Cell **12:** 803–816

Ron M, Avni A (2004) The receptor for the fungal elicitor ethylene-inducing xylanase is a member of a resistance-like gene family in tomato. Plant Cell **16:** 1604–1615

Sanders D, Pelloux J, Brownlee C, Harper JF (2002) Calcium at the crossroads of signaling. Plant Cell (Suppl) **14:** S401–S417

Shi J, Kim KN, Ritz O, Albrecht V, Gupta R, Harter K, Luan S, Kudla J (1999) Novel protein kinases associated with calcineurin B-like calcium sensors in *Arabidopsis*. Plant Cell **11:** 2393–2405

Shimizu T, Jikumaru Y, Okada A, Okada K, Koga J, Umemura K, Minami E, Shibuya N, Hasegawa M, Kodama O, et al (2008) Effects of a bile acid elicitor, cholic acid, on the biosynthesis of diterpenoid phytoalexins in suspension-cultured rice cells. Phytochemistry **69:** 973–981

Su W, Wu J, Wei C, Li K, He G, Attla K, Qian X, Yang J (2006) Interaction

between programmed cell death 5 and calcineurin B-like interacting protein kinase 23 in *Oryza sativa*. Plant Sci **170:** 1150–1155

Takabatake R, Karita E, Seo S, Mitsuhara I, Kuchitsu K, Ohashi Y (2007) Pathogen-induced calmodulin isoforms in basal resistance against bacterial and fungal pathogens in tobacco. Plant Cell Physiol **48:** 414–423

Tanaka H, Kayano T, Ugaki M, Shiobara F, Onodera H, Ono K, Tagiri A, Nishizawa Y, Shibuya N, inventors. February 1, 2001. Ultra-fast transformation technique for monocotyledons. International Patent Publication No. WO 01/06844 A1

Turner JG, Novacky A (1974) The quantitative relation between plant and bacterial cells involved in the hypersensitive reaction. Phytopathology **64:** 885–890

Umemura K, Ogawa N, Koga J, Iwata M, Usami H (2002) Elicitor activity of cerebroside, a sphingolipid elicitor, in cell suspension cultures of rice. Plant Cell Physiol **43:** 778–784

Waadt R, Schmidt LK, Lohse M, Hashimoto K, Bock R, Kudla J (2008) Multicolor bimolecular fluorescence complementation reveals simultaneous formation at alternative CBL/CIPK complexes *in planta*. Plant J **56:** 505–516

Xiang Y, Huang Y, Xiong L (2007) Characterization of stress-responsive *CIPK* genes in rice for stress tolerance improvement. Plant Physiol **144:** 1416–1428

Yamada A, Shibuya N, Kodama O, Akatsuka T (1993) Induction of phytoalexin formation in suspension-cultured rice cells by *N*-acetylchitooligosaccharides. Biosci Biotechnol Biochem **57:** 405–409

Yamakawa H, Mitsuhara I, Ito N, Seo S, Kamada H, Ohashi Y (2001) Transcriptionally and post-transcriptionally regulated response of 13 calmodulin genes to tobacco mosaic virus-induced cell death and wounding in tobacco plant. Eur J Biochem **268:** 3916–3929

Yamamoto Y, Kobayashi Y, Devi SR, Rikiishi S, Matsumoto H (2002) Aluminum toxicity is associated with mitochondrial dysfunction and the production of reactive oxygen species in plant cells. Plant Physiol **128:** 63–72

Yang T, Poovaiah BW (2003) Calcium/calmodulin-mediated signal network in plants. Trends Plant Sci **8:** 505–512

Yao N, Eisfelder BJ, Marvin J, Greenberg JT (2004) The mitochondrion—an organelle commonly involved in programmed cell death in *Arabidopsis thaliana*. Plant J **40:** 596–610

Yoshioka H, Asai S, Yoshioka M, Kobayashi M (2009) Molecular mechanisms of generation for nitric oxide and reactive oxygen species, and role of the radical burst in plant immunity. Mol Cells **28:** 321–329

Zhu JK (2002) Salt and drought stress signal transduction in plants. Annu Rev Plant Biol **53:** 247–273

Zielinski RE (1998) Calmodulin and calmodulin-binding proteins in plants. Annu Rev Plant Physiol Plant Mol Biol **49:** 697–725

Zielinski RE (2002) Characterization of three new members of the *Arabidopsis thaliana* calmodulin gene family: conserved and highly diverged members of the gene family functionally complement a yeast calmodulin null. Planta **214:** 446–455